Febrary 2009

SLAC-PUB-13533

Generating intense attosecond x-ray pulses using ultraviolet-laser-induced microbunching in electron beams

D. Xiang, Z. Huang and G. Stupakov

SLAC National Accelerator Laboratory,

Stanford University, Stanford, California, 94309, USA

Abstract

We propose a scheme that combines the echo-enabled harmonic generation technique with the bunch compression and allows to generate harmonic numbers of a few hundred in a microbunched beam through up-conversion of the frequency of an ultraviolet seed laser. Sending this beam through a short undulator results in an isolated sub-100 attoseconds pulse of x-ray radiation. Using a representative realistic set of parameters, we show that 1 nm x-ray pulse with peak power exceeding 100 MW and duration as short as 34 attoseconds (FWHM) can be generated from a 200 nm ultraviolet seed laser.

Submitted to Phys. Rev. Lett.

Work supported by US DOE contracts DE-AC02-76SF00515.

Fast time-dependent phenomena are typically studied with pump-probe technique in which the dynamics are initiated by a pump laser and then probed by a delayed pulse. The advent of attosecond (as) pulses made possible the time-resolved study of the electronic dynamics which opened up many new ultrafast sciences [1-5]. Using the ~ 100 as soft x-ray pulse in the wavelength ~ 10 nm, the inner-shell atomic process was traced in [2] and the time required for an electron to travel from one atom to another was studied in [3]. Most recently the pulse duration has been pushed to about 80 as in the extreme ultraviolet wavelength [5]. These studies all relied on the technique of high harmonic generation in gas where an intense laser pulse was focused on an atomic gas jet and the high harmonic of the laser was generated and further used as the probe. However, it appears difficult to generate intense harmonic radiation with wavelength down to 1 nm or shorter with this technique.

To achieve atomic spatial resolution, the radiation wavelength needs to be pushed to ~ 1 nm or shorter, and the isolated attosecond pulse is also highly desirable. There is a growing trend to provide such attosecond x-ray pulse using free electron lasers (FEL) [6-15]. Most of the proposed schemes utilized intense lasers to manipulate the electron beam energy and then selected a small part of the electrons to lase [8-13]. The schemes [7,9-14] that use self-amplified spontaneous emission (SASE) to generate attosecond x-ray pulse may suffer from statistic fluctuations because SASE originates from electron beam shot noise. An alternative scheme [8] which overcomes this problem is to use the high gain harmonic generation (HGHG) configuration. But due to the relatively low up-frequency conversion efficiency, the HGHG scheme requires an intense seed signal in the wavelength of a few nm which is in principle obtainable but does not exist today.

In this paper, we propose a novel scheme which allows to generate intense isolated attosecond x-ray in the wavelength ~ 1 nm or shorter based on existed technologies. The scheme combines the echo-enabled harmonic generation (EEHG) technique [16,17] with the bunch compression technique and allows harmonic numbers of a few hundred to be accessible that eventually enables the generation of x-ray radiation from an ultraviolet (UV) seed laser. The required energy chirp in the bunch compression is provided by a few-cycle intense infrared (IR) laser which finally assists in generation of an isolated attosecond x-ray pulse. Using a representative realistic set of parameters, we show that 1 nm isolated x-ray pulse with duration of about 34 as (FWHM) and peak power exceeding 100 MW can be generated in a short radiator with only 20 undulator periods using the proposed scheme. Since the

generated attosecond x-ray pulse is in tight synchronization with the few-cycle laser, it is straightforward to use them for ultrafast pump-probe experiments.

Our scheme requires an ultrarelativistic electron beam, a UV seed laser, a few-cycle intense IR laser, together with four undulator sections and two dispersion sections. The wavelength of the UV seed laser is assumed to be 200 nm and that of the few-cycle IR laser is 800 nm. We further assume that the lasers originate from the same Ti:Sapphire oscillator which will allow tight synchronization between them. The schematic of the proposed scheme is shown in Fig.1.

The first part of the proposed scheme is similar to the EEHG FEL [16,17] in which the beam is energy modulated in the first modulator (M1) and then sent through a dispersion section with strong dispersion strength $R_{56}^{(1)}$ after which the modulation obtained in M1 is macroscopically washed out while simultaneously complicated fine structures (separated energy bands) are introduced into the phase space of the beam. In the EEHG scheme, a second laser is used to further modulate the beam energy in the second modulator (M2). After passing through the second dispersion section with dispersion strength $R_{56}^{(2)}$, the separated energy bands will convert to separated current bands and the echo signal then occurs as a recoherence effect caused by the mixing of the correlations between the modulation in the second modulator and the fine structures.

In our proposed scheme for generation of an isolated attosecond x-ray pulse, we introduce an extra modulator (M3) between M2 and the second dispersion section. The beam interacts in M3 with a few-cycle intense laser of which the wavelength is chosen to be much longer than that of the laser in M2, so that part of the electrons around the zero crossing of the few-cycle laser gets almost linear energy chirp. With this additional energy chirp, the beam is longitudinally compressed after passing through the second dispersion section and the harmonic number is increased by the compression factor. As we will show below, in addition

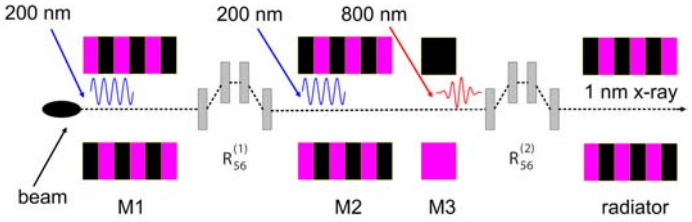

FIG. 1: Schematic of the proposed scheme for generation of isolated attosecond x-ray pulse.

to assisting in extension of the harmonic number to a few hundred, the few-cycle laser also offers a possibility to select an isolated attosecond pulse.

We assume an initial Gaussian beam energy distribution with an average energy E_0 and the rms energy spread σ_E, and use the variable $p = (E - E_0)/\sigma_E$ for the dimensionless energy deviation of a particle. The initial normalized distribution function of the beam is $f_0(p) = N(2\pi)^{-1/2}e^{-p^2/2}$, where N is the number of electrons per unit length of the beam. After passing through M1, the beam energy is modulated with the amplitude ΔE_1, so that the final dimensionless energy deviation p' is related to the initial one p by the equation $p' = p + A_1 \sin(kz)$, where $A_1 = \Delta E_1/\sigma_E$, z is the longitudinal coordinate in the beam, k is the wave number of the laser, and in our example we assume the laser wavelength of 200 nm. Sending the beam through the first dispersion section with the dispersion strength $R_{56}^{(1)}$ converts the longitudinal coordinate z into z', $z' = z + R_{56}^{(1)} p\sigma_E/E_0$, and the resulting distribution function is [16,17],

$$f_1(\zeta, p) = \frac{N}{\sqrt{2\pi}} \exp\left[-\frac{1}{2}\left(p - A_1 \sin(\zeta - B_1 p)\right)^2\right], \tag{1}$$

where $\zeta = kz$, $B_1 = R_{56}^{(1)} k\sigma_E/E_0$. The beam is then energy modulated in M2 with the dimensionless modulation amplitude A_2. Assuming the laser wavelength to be the same, at the exit of M2 the beam longitudinal phase space evolves to,

$$\begin{aligned} f_2(\zeta, p) = \frac{N}{\sqrt{2\pi}} \exp\Big[-\frac{1}{2}\big(p - A_2 \sin\zeta \\ - A_1 \sin(\zeta - B_1(p - A_2 \sin\zeta))\big)^2\Big], \end{aligned} \tag{2}$$

Before entering the second dispersion section, the beam is further energy modulated in M3 with an intense, few-cycle laser for which the wavelength is much longer than that in the upstream modulators. The carrier-envelope phase of the few-cycle laser pulse is set to $\pi/2$ so that the oscillating electric field is zero at the pulse peak [18]. A snapshot of the 800 nm few-cycle laser field normalized to the peak value is shown in Fig.2a.

To show how the few-cycle laser assists in generation of much higher harmonic and an isolated attosecond x-ray pulse, we add a linear energy chirp to the beam distribution before sending the beam to the second dispersion section. Assuming the linear energy chirp factor is $h = dp/d\zeta$, the resulting longitudinal phase space distribution at the exit from the second

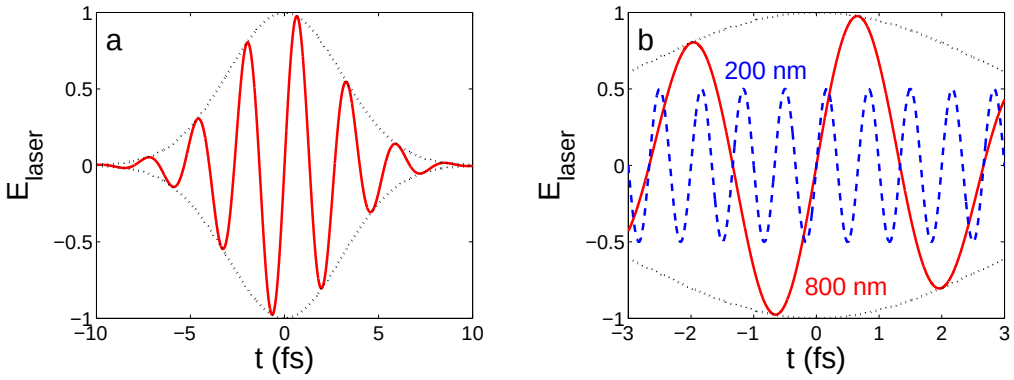

FIG. 2: (a) A snapshot of the laser field normalized to the peak value for the 800 nm few-cycle laser with pulse length 5 fs (FWHM of intensity); (b) Schematic of the synchronization between the laser in M2 and the few-cycle laser (laser field not in scale).

dispersion section is,

$$f_3(\zeta,p) = \frac{N}{\sqrt{2\pi}}\exp\Big[-\frac{1}{2}\big((1+hB_2)p - A_2\sin(\zeta - B_2p) - h\zeta - A_1\sin[(1+hB_1)\zeta + A_2B_1\sin(\zeta - B_2p) - (B_1+B_2+hB_1B_2)p]\big)^2\Big], \tag{3}$$

where $B_2 = R_{56}^{(2)}k\sigma_E/E_0$. Integration of Eq.(3) over p yields the final current distribution which can be expanded in Fourier series,

$$b(\zeta) = CN\left[1 + 2\sum_{n=1}^{\infty} b_n\cos(Cn\zeta + \psi_n)\right], \tag{4}$$

The wave number of the echo signal is Cnk, where $C = 1/(1+hB_2)$ is the compression factor and the corresponding maximized bunching factor for this harmonic radiation is,

$$b_n = |J_{n+1}(CnA_2B_2)\,J_1(A_1(CnB_2 - B_1))| \exp\left[-\frac{1}{2}(CnB_2 - B_1)^2\right], \tag{5}$$

The bunching factor at the harmonic number m is defined as $\langle e^{imkz}\rangle$, where mk is the wave number of the harmonic radiation and the brackets denote averaging over the longitudinal coordinate z. A comparison between this equation and Eq.(6) in Ref.[17] indicates that for given energy modulation amplitudes the bunch compression extends the harmonic number by a factor of C while keeping the value of the bunching factor unchanged. Assuming a compression factor of 5 and relatively small energy modulation amplitudes in the

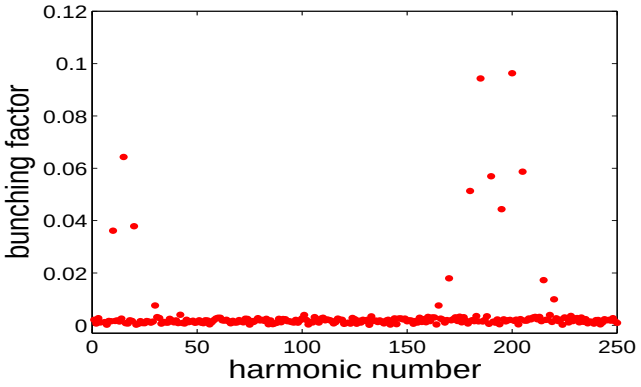

FIG. 3: Bunching factors for various compressed harmonic numbers Cn.

two modulators, $A_1 = A_2 = 3$, with the method described in Ref.[17], we find that the dispersion strengths and the chirp factor which maximize the bunching factor of the 200th harmonic ($n = 40$) are $B_1 \approx 14.080$, $B_2 \approx 0.073$ and $h \approx -10.961$, respectively. With these parameters, the electrons are tracked through the modulators and dispersion sections and the bunching factors for various harmonic numbers are calculated from definition and shown in Fig.3 where it can be seen that the bunching factor for the 200th harmonic (1 nm wavelength for a 200 nm seeding laser) is about 0.1. Sending this prebunched beam to the radiator will generate powerful coherent x-ray at 1 nm wavelength.

To show the feasibility of the proposed scheme in generating an attosecond x-ray pulse, we consider an ultrarelativistic electron beam with energy of 3 GeV, peak current of 1 kA, normalized emittance of 1 μm and slice energy spread of 150 keV. The undulator period length and number of periods are assumed to be 25 cm and 6 in both M1 and M2. A 200 nm laser with peak power $\sim$ 100 MW is used to modulate the beam in M1 and M2 with the peak-to-peak energy modulation amplitude of 900 keV. The strength of the two dispersion sections are 8.964 mm and 0.046 mm, respectively. These modulations and dispersions correspond to $A_1 = A_2 = 3$, $B_1 = 14.080$ and $B_2 = 0.073$. An 800 nm few-cycle laser with energy $\sim$ 1 mJ and pulse length of 5 fs (FWHM) is used to modulate the beam in M3. The undulator period length is assumed to be 20 cm for M3 and it has only one period. To take advantage of the bunch compression assisted harmonic generation, the few-cycle laser is time delayed to make its zero crossing overlap with that of the UV laser in M2, as is shown in Fig.2b. Because the wavelength of the few-cycle laser is much longer than that of the UV laser in M2, the electrons in the regions around the zero crossings get almost linear energy

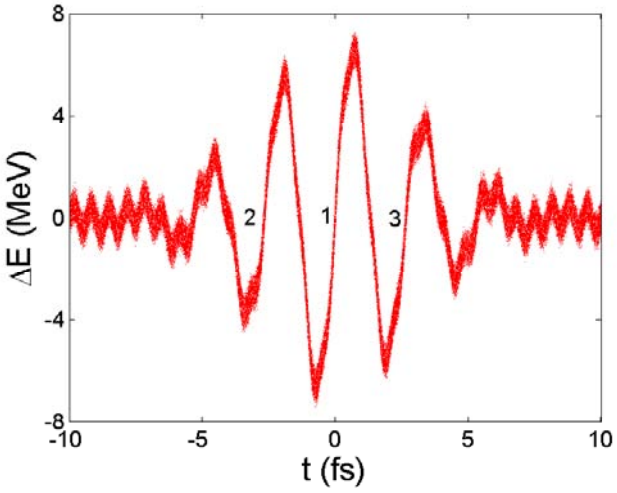

FIG. 4: Longitudinal phase space of the beam after interaction with the few-cycle laser (bunch head at left).

chirp which allows longitudinal compression after passing through a dispersive element. The longitudinal phase space of the beam after interaction with the few-cycle laser is shown in Fig.4.

From Fig.4 it follows that there are three regions where electrons have almost linear negative energy chirp: the region around the zero crossing of the central cycle ($t = 0$, region 1 in Fig.4) and those around the zero crossings of the nearest side cycles($t = \pm 2.67$ fs, region 2 and 3 in Fig.4). The fine structure of the longitudinal phase space for the electrons at region 1 and region 2 is shown in Fig.5a and Fig.5b (the electrons in region 3 are similar to those in region 2). It can be easily seen that the energy chirp factor for the electrons in region 2 are approximately 1.5 times smaller than those in region 1. The laser power is adjusted in such a way that only electrons in region 1 have the correct chirp factor ($h \approx -10.961$) to maximize the 200th harmonic of the seed laser. With these conditions the longitudinal phase space of the electrons in these regions after passing through the second dispersion section are shown in Fig.5c and Fig.5d.

As can be seen in Fig.5, the separated energy bands in the central cycle effectively convert to separated current bands which contain considerable higher harmonic components while those in the side cycles fail to convert to 'upright' bands due to the small chirp factor. The bunching factor at 1 nm wavelength for the central slice is about 0.1 and that for all other slices is at the shot noise level, which makes possible the generation of an isolated attosecond

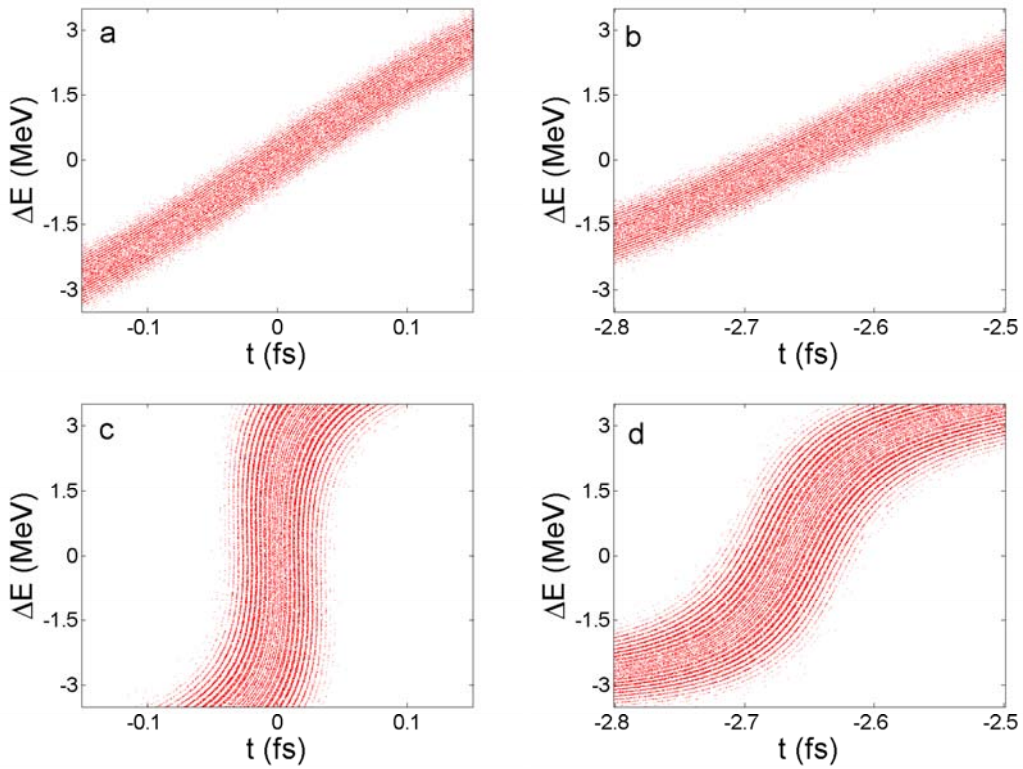

FIG. 5: Longitudinal phase space at the exit from M3 for the electrons in region 1-(a) and those in region 2-(b); Longitudinal phase space at the entrance to the radiator for the electrons in region 1-(c) and those in region 2-(d).

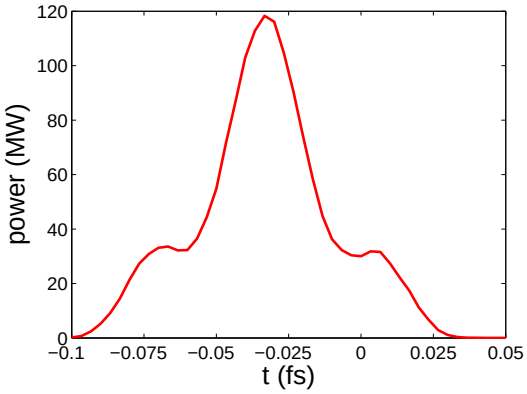

FIG. 6: Power of the generated 1 nm x-ray pulse. The pulse length is 34 as (FWHM).

x-ray pulse. The current of the central slice is also enhanced by a factor of 5 from the bunch compression. It can be expected that intense 1 nm x-rays will be generated after sending this prebunched, high-peak-current beam slice through the radiator.

The output radiation field may be calculated by summing up the field of each electron

in the radiator. The output x-ray pulse length is determined by both the electron bunch length and the slippage length in the undulator. For the SASE schemes [7,9-14], the slippage length associated with the long FEL undulator typically limits the radiation pulse length to a few hundred attoseconds. Since in our scheme a short section of the beam is effectively prebunched at the radiator entrance, only a short undulator is required to generate intense x-rays which may allow pushing the pulse length to sub-100 as. In our example, we used a planar undulator with $N_u = 20$ periods and the period length $\lambda_u = 4$ cm to generate $\lambda_r = 1$ nm x-rays. We further assumed that the relative longitudinal position of the electrons did not change during the passage through the short radiator, which was justified for an electron beam with 1 μm normalized emittance and a transverse rms size $\sigma_x = 20$ μm. For these parameters, the single-electron undulator radiation has a rms transverse size $\sqrt{2\lambda_r\lambda_u N_u}/(4\pi) \ll \sigma_x$ and can be approximated as a plane wave. Thus the output power can be calculated as (see for example [19])

$$P(t) = \frac{e^2c^2Z_0K^2[\mathrm{JJ}]^2\lambda_u^2}{32\pi\sigma_x^2\gamma_0^2\lambda_r^2}\Big|\sum_j e^{-i2\pi c(t_j-t)/\lambda_r}\Big|^2, \tag{6}$$

where $Z_0 = 377\ \Omega$ is the vacuum impedance, K is the undulator parameter, $[\mathrm{JJ}] = J_0(\xi) - J_1(\xi)$ is the usual Bessel function factor associated with the planar undulator, $\xi = K^2/(4 + 2K^2)$, $E_0 = \gamma_0 mc^2$ is the beam energy, and the sum over jth electron is carried out within the radiation slippage length, i.e. $0 < c(t_j - t) < N_u\lambda_r$. Using the beam distribution at the radiator entrance, the power profile of the x-ray radiation at 1 nm wavelength generated in the radiator is shown in Fig.6. The peak power exceeds 100 MW, and the pulse length is 34 as (FWHM) approaching the atomic unit of time (24 as). It is worth pointing out that the bunching factor depends on the energy chirp factor which varies if the IR laser energy changes. In order to keep the fluctuation of the output x-ray power smaller than 10%, the laser energy fluctuation should be controlled to be within 1%.

In conclusion, we have proposed a scheme to extend the harmonic numbers to a few hundred that eventually enables the generation of an intense isolated attosecond x-ray pulse from a UV seed laser. It is capable of breaking the 100-as time barrier and may open a new regime of ultrafast sciences.

We thank A. Chao, Y. Ding, D. Ratner and J. Wu for helpful discussions. This work was

supported by the US DOE under Contract No. DE-AC02-76SF00515.

---

[1] P.M. Paul, *et al.*, Science 292, 1689 (2001).

[2] M. Hentschel, *et al.*, Nature(London) 414, 509 (2001).

[3] A. Föhlisch, *et al.*, Nature(London 436, 373 (2005).

[4] P.B. Corkum and Ferenc Krausz, Nature Phys. 3, 381 (2007).

[5] E. Goulielmakis, *et al.*, Science 320, 1614 (2008).

[6] E.L. Saldin, E.A. Schneidmiller, and M.V. Yurkov, Opt. Commun. 212, 377 (2002).

[7] P. Emma, *et al.*, Phys. Rev. Lett, 92, 074801 (2004).

[8] A.A. Zholents and W.M. Fawley, Phys. Rev. Lett, 92, 224801 (2004).

[9] E.L. Saldin, E.A. Schneidmiller, and M.V. Yurkov, Opt. Commun. 239, 161 (2004).

[10] A.A. Zholents and G. Penn, Phys. Rev. ST Accel. Beams, 8, 050704 (2005).

[11] E.L. Saldin, E.A. Schneidmiller, and M.V. Yurkov, Phys. Rev. ST Accel. Beams, 9, 050702 (2006).

[12] Y. Ding, *et al.*, SLAC-PUB-13393, (2008).

[13] A.A. Zholents and M.S. Zolotorev, New J. Phys, 10, 025005 (2008).

[14] S. Reiche, et al., Nucl. Instrum. Methods Phys. Res., Sect. A 593, 45 (2008).

[15] N.R. Thompson and B.W.J. McNeil, Phys. Rev. Lett, 100, 203901 (2008).

[16] G. Stupakov, Phys. Rev. Lett, to be published; see also SLAC-PUB-13445 (2008).

[17] D. Xiang and G. Stupakov, SLAC-PUB-13474 (2008).

[18] A. Baltuška, *et al.*, Nature(London) 421, 611 (2003).

[19] Z. Huang and K. Kim, in *Proceedings of the 1999 Particle Accelerator Conference* (New York, 1999), p2495.